Pharmaceutical Research, Vol. 25, No. 12, December 2008 (© 2008)
DOI: 10.1007/s11095-008-9653-9

Research Paper

Ultrasound Assisted Engineering of Lactose Crystals

Ravindra S. Dhumal,[1] Shailesh V. Biradar,[1] Anant R. Paradkar,[1,2,3] and Peter York[2]

Received April 22, 2008; accepted June 4, 2008; published online July 1, 2008

Purpose. To engineer lactose crystals of desired size, shape, surface and particle size distribution (PSD) as a carrier for dry powder inhalers (DPI) by ultrasound assisted *in-situ* seeding.
Methods. Lactose crystals were obtained from solution by ultrasound assisted *in-situ* seeding, followed by growth in viscous glycerin solution. The crystals were characterized for physical properties and 63–90 μm size fractions of different batches were mixed with salbutamol sulphate (SS) and compared for *in-vitro* deposition.
Results. Cooling crystallization with stirring for 10–20 h resulted in crystals with wide PSD and varied shape. Application of ultrasound resulted in rapid and complete crystallization in 5 min with rod-shaped fine crystals (15–30 μm) and narrow PSD. *In-situ* seeded batches yielded micro-fine rod-shaped seed crystals. Seeding followed by growth in glycerin showed desirable size, high elongation ratio, smooth surface and narrow PSD, while growth under stirring showed high elongation ratio with rough surface. Crystals grown in glycerin showed highest dispersibility and fine particle fraction (FPF) of SS.
Conclusions. Ultrasound assisted *in-situ* seeding, followed by ordered growth in glycerin offers rapid technique for separation of nuclei induction from crystal growth yielding desirable characteristics for better dispersion and *in-vitro* deposition when employed as DPI carrier.

KEY WORDS: dry powder inhaler; particle engineering; ultrasound assisted crystallization; α-lactose monohydrate.

INTRODUCTION

Lactose, 4-(β-D-galactosido-)-D-glucose is commercially produced from the whey of cows' milk. After heat-induced deproteination, the residual whey is concentrated and cooled to yield raw lactose (1,2), which is re-dissolved, charcoal treated and recrystallized (1,3). Crystal habit of lactose varies from prism, pyramid to tomahawk depending on conditions of crystallization (4). Above 93.5°C β-lactose anhydrous is formed, while below this, α-lactose monohydrate (α-LM) is obtained (5). The main drawback of conventional cooling crystallization is long induction time and slow crystallization rate extending up to 72 h (1). This is due to large metastable zone width, which require very high supersaturation for induction to occur (6). Attempts for rapid crystallization of lactose include seeding crystallization (7,8), anti-solvent precipitation using ethanol (9,10), methanol (11), DMSO (12), acetone (13) and sonocrystallization (14). Nature and time of seed addition affects the crystal habit limiting the applicability and reproducibility of process (15,16). During anti-solvent process, mechanical agitation provides mainly macroscopic mixing of anti-solvent molecules in solution, generating few local zones of excessive supersaturations leading to heterogeneous growth and agglomeration (17). Bund and Pandit, has reported application of ultrasound during anti-solvent crystallization of lactose for achieving

[1] Department of Pharmaceutics, Bharati Vidyapeeth University, Poona College of Pharmacy and Research Centre, Erandawane, Pune 411038, Maharashtra, India.
[2] Institute of Pharmaceutical Innovations, University of Bradford, Bradford, West Yorkshire BD7 1DP, UK.
[3] To whom correspondence should be addressed. (e-mail: arparadkar@rediffmail.com)

ABBREVIATIONS: *A*, area; ρ_{bulk}, bulk density; CC-1, cooling crystallization from lactose solution 30% *w*/*w*; CC-2, cooling crystallization from lactose solution 40% *w*/*w*; CC-3, cooling crystallization from lactose solution 50% *w*/*w*; CI, Carr's index; DPI, dry powder inhaler; DSC, differential scanning calorimetry; ED, emitted dose; FPD, fine particle dose; FPF, fine particle fraction; ΔH_d, enthalpy of dehydration of lactose obtained from the dehydration endotherm (J/g); ΔH_v, enthalpy of vaporization of water, 2,261 J/g; *L*, length; α-LM, α-lactose monohydrate; *P*, perimeter; PSD, particle size distribution; RD, recovered dose; $RMM_{lactose}$, molecular mass of anhydrous lactose (340.3); RMM_{water}, molecular mass of water (18.0); SEM, scanning electron microscopy; Sono-1, crystallization of 30% *w*/*w* lactose solution with sonication for 5 min; Sono-2, crystallization of 40% *w*/*w* lactose solution with sonication for 5 min; Sono-3, crystallization of 50% *w*/*w* lactose solution with sonication for 5 min; Sono-G1, crystallization of 30% *w*/*w* lactose solution with sonication for 45 s followed by growth in glycerin; Sono-G2, crystallization of 40% *w*/*w* lactose solution with sonication for 45 s followed by growth in glycerin; Sono-G3, crystallization of 50% *w*/*w* lactose solution with sonication for 45 s followed by growth in glycerin; Sono-S1, crystallization of 30% *w*/*w* lactose solution with sonication for 45 s followed by stirring; Sono-S2, crystallization of 40% *w*/*w* lactose solution with sonication for 45 s followed by stirring; Sono-S3, crystallization of 50% *w*/*w* lactose solution with sonication for 45 s followed by stirring; SS, salbutamol sulphate; ρ_{tap}, tap density; TGA, thermogravimetric analysis; *W*, width; XRPD, X-ray powder diffractometry.

0724-8741/08/1200-2835/0 © 2008 Springer Science + Business Media, LLC

homogeneous supersaturation throughout crystallization vessel, resulting in rapid recovery of non-agglomerated fine lactose crystals (5–10 μm) (14).

The crystal habit of α-LM a widely used pharmaceutical excipient (5) influences its functionality and downstream processing in variety of pharmaceutical dosage forms. In particular, when employed as carrier for dry powder aerosols to overcome intrinsic cohesiveness of micronized drug particles (18). Drug delivery from these interactive mixtures is known to be influenced by particles size, shape and surface (19–21). Particles with average size in the range of 63–90 μm, smooth surfaces and high elongation ratio exhibit better dispersibility and FPF (19,22). Faster anti-solvent crystallization in known to accelerate the growth of length at the expense of width and thickness resulting in elongated but fine crystals (5–10 μm). These crystals are not suitable as carrier for DPI. In contrast, lactose crystals grow to maturity without surface defect during crystallization from carbopol gel resulting in large regular crystals with smooth surface and improved FPF (22,23). However, longer crystallization time (72 h), low yield and tedious harvesting process limit its application. Lactose crystallization from glycerin is also reported to show smooth surface without much of the drawbacks associated with gels (24).

As spontaneous nucleation occurs at high levels of supersaturation and lower levels favor slow and ordered growth into large crystals, ideal experiment must somehow separate nucleation from growth to satisfy distinctly different requirements of these two events. Therefore, it's a challenge to develop rapid crystallization process to yield lactose crystals with desirable size, shape and surface for DPI application. Sonocrystallization has been used advantageously to replace conventional seeding to generate extremely small seed crystals rapidly and easily (25) for drugs (17), high energy materials (26) and organic solids (16) without drawbacks of conventional seeding. Nuclei induction by ultrasound during cooling crystallization results in large crystals (16). In our previous attempt, we have obtained porous and sintered particles by melt sonocrystallization, but it is not always possible to process the melt without degradation (27,28).

However, it is possible to achieve ultrasound assisted spontaneous *in-situ* seeding during cooling crystallization while growing the micro-fine seed crystals steadily in stagnant viscous glycerin solution. As glycerin is miscible in both water and ethanol the crystals could be harvested easily by washing with ethanol/water mixture. This was done with the aim of engineering lactose crystals with desirable size (63–90 μm), regular shape, smooth surface and narrow PSD for application as carrier for dry powder aerosols.

MATERIALS AND METHODS

MATERIALS

α-Lactose monohydrate (Pharmatose 200 M, DMV International, The Netherlands), hard gelatin capsules (Universal Capsules, Mumbai, India), micronized salbutamol sulphate and Rotahaler® (Cipla Ltd, Mumbai, India) were received as gift sample. Ethanol (analytical grade) and glycerin (general reagent) were purchased from Merck, India.

Crystallization

Crystallization of lactose from aqueous solutions was carried out by cooling with application of ultrasound energy using a probe and sonifier (Sonics and materials Inc., Vibra Cell, Model VCX 750, CT, USA) operating at a fixed wavelength of 20 kHz and capable of inducing a maximum power output of 750 W. Probe (tip diameter 13 mm) was immersed 5 mm in the processing liquid. The lactose solutions (30% *w*/*w*, 40% *w*/*w* and 50% *w*/*w*) were prepared by dissolving α-LM in 100 ml water at 90°C and filtered through 0.45 μm pore size membranes. The solutions were transferred to a 500 ml jacketed crystallization vessel having constant speed stirrer with propeller having three-blades (1×3 cm) (Eurostar power control-visc, IKA Labortecnik, Germany) which was situated 2 cm above the bottom of vessel. The solutions were allowed to cool down from 90°C to 25°C by circulating water maintained at 20°C using cryostatic bath (Haake Phoenix C25P, Germany) in the jacket. The cooling time varies from 220 to 240 min. For batches Sono-1, Sono-2 and Sono-3, α-LM solutions were sonicated for 5 min. Whereas, Sono-S1, Sono-S2 and Sono-S3 were prepared by sonication for 45 s, followed by stirring at 500 rpm. Sono-G1, Sono-G2 and Sono-G3 were sonicated for 45 s, followed by addition of glycerin to achieve 20% *w*/*w* solution. For control batches CC-1, CC-2 and CC-3, the solutions were cooled down to 40°C by circulating water maintained at 40°C in the jacket. The cooling time varies from 155 to 170 min. In these batches, solutions were agitated at 500 rpm without sonication. The crystallization time and summary of experimental conditions of various batches are specified in Table I.

After crystallization has been allowed to continue for a predetermined period of time, the crystals were separated by filtration and washed with 60% (*v*/*v*) ethanol followed by 100% ethanol. The crystals were allowed to dry at room temperature overnight before drying in a vacuum oven at 70°C for 3 h. A small amount of sample was taken from each batch of lactose for the micromeritic and polymorphic evaluation. The remaining lactose crystals were then poured into a 90 μm sieve that had been placed upon a 63 μm sieve (Jayant test sieves, Mumbai, India). The particles were then sieved manually into three size fractions (<63, 63–90 and >90 μm), which were collected and weighed separately. The lactose fractions thus obtained were transferred separately to vials, sealed and placed into a desiccator over silica gel.

Micromeritic Properties

Particle Size Distribution

Particle size was measured by Laser Diffractometer, Mastersizer 2000 Ver. 2.00 (Malvern Instruments, Malvern, UK). Analysis was done in triplicate and mean results are presented. Ethanol was used as dispersant and obscuration was not less than 10% for each measurement. Data analysis was done by Malvern Software Ver 5.2.

Image Analysis

The images were captured using a stereomicroscope (Carl Zeiss, Germany) attached with a digital camera (WAT-

Table I. Summary of Experimental Conditions, Percent Yield, D_{90}, Span and PSD of Different Lactose Batches

Batch code	Lactose conc. (% *w/w*)	Sonication time	Appearance of turbidity	Post sonication treatment	Total time of crystallization (min/hr)	% yield	D_{90} (μm)[a]	Span[a]	% particles (μm)[b]		
									<63	63–90	<90
CC-1	30	NA	10 h	NA	20 h (stirring)	44	101	2.2	23	33	44
CC-2	40		8 h		12 h (stirring)	48	93	2.1	27	35	38
CC-3	50		3 h		8 h (stirring)	53	86	2.1	37	27	36
Sono-1	30	5 min	30 s	NA	5 min	83	27	1.1	100	–	–
Sono-2	40					84	22	1.3	100	–	–
Sono-3	50					84	15	1.4	100	–	–
Sono-S1	30	45 s	30 s	Stirring	3 h	76	80	1.4	30	42	27
Sono-S2	40					78	79	1.5	28	41	30
Sono-S3	50					79	78	1.6	26	41	33
Sono-G1	30	45 s	30 s	Growth in 20% *w/w* glycerin	5 h	74	81	1.2	9	55	36
Sono-G2	40					75	80	1.2	10	55	35
Sono-G3	50					76	79	1.1	10	54	36

[a] Determined by Malvern Mastersizer
[b] Sieve analysis data

202, Watec, Japan). The captured images were analyzed using Biovis Image Plus software (Expert Tech Vision, India) by method reported earlier (29). Fifty crystals were measured in each sample and the length (L), width (W), perimeter (P), and area (A) were recorded. Different shape descriptors like shape factor, surface factor and elongation ratio (E) were derived as follows.

$$\text{Elongation ratio} = L/W \tag{1}$$

$$\text{Shape factor} = 4\pi \times A/P^2 \tag{2}$$

$$\text{Surface Factor} = \text{Surface factor} \times (1+E)^2 \Big/ (\prod \times E) \tag{3}$$

E has a value in the range >1, higher the value more elongated the particle. The shape factor is a two-dimensional shape descriptor used in many image analysis software programs and combines properties related to both surface roughness and shape. A spherical particle with smooth surface will have a shape factor of 1, whilst non-spherical particles or spherical particles with a rough surface will have a shape factor value between 0 and 1. The more irregular the shape and/or rougher the surface, smaller is the shape factor. Surface factor is a derived factor which also varies from 0–1 but is primarily dependent upon surface roughness alone; particles that are perfectly smooth would have a value of 1.

Surface Topography

Surface topography was characterized using scanning electron microscopy (SEM). Freshly prepared samples were mounted on the aluminum stub and coated with a thin gold–palladium layer by Auto fine coater (Jeol, JFC, Tokyo, Japan) and analyzed with a scanning electron microscope (Jeol, JSM-6360, Tokyo, Japan) operated at an 10 kV acceleration voltage.

Powder Flow

Carr's Index

The static powder flow was characterized using Carr's compressibility index (CI), determined from the tap (ρ_{tap}) and bulk densities (ρ_{bulk}) using following formula:

$$\text{CI} = \frac{\rho_{tap} - \rho_{bulk}}{\rho_{tap}} * 100 \tag{4}$$

Bulk density was determined by filling the powder in a 10 ml measuring cylinder and tap density was measured using tap density tester (ETD-1020, Electrolab, Mumbai, India) following 500 taps, which allowed the density plateau. Lower CI values are indicative of better flow behavior.

Angle of Repose

The dynamic powder flow was characterized using angle of repose. Lactose crystals were carefully poured into a glass funnel which had been placed over a flat base. After the powder column reached a height of approximately 4 cm, the

addition of powder was stopped and the funnel was slowly lifted, leaving a cone of powder. The height of the cone was measured and the angle of repose was calculated from the tangent (cone height/cone base radius). Each sample was measured in triplicate.

Characterization of Polymorphic Form

Thermogravimetric Analysis (TGA)

Samples (approximately 30–40 mg) were heated at a constant rate of 10°C/min over a temperature range of 25–220°C in platinum crucibles. Inert atmosphere was maintained by purging nitrogen gas at flow rate of 50 ml/min and the loss of mass as a function of temperature was recorded using TA-60WS Thermogravimetric analyzer (Shimandzu, Japan).

Differential Scanning Calorimetry (DSC)

DSC studies were carried out using Mettler-Toledo DSC 821^e instrument equipped with an intracooler (Mettler-Toledo, Switzerland). Indium and zinc standards were used to calibrate the DSC temperature and enthalpy scale. The samples were hermetically sealed in aluminum crucibles and heated at a constant rate of 10°C/min over a temperature range of 25–220°C. Inert atmosphere was maintained by purging nitrogen gas at flow rate of 50 ml/min.

X-ray Powder Diffraction (XRPD)

The XRPD patterns were recorded on X-ray diffractometer (D8 Advance, Bruker AXS Inc, Madison, USA). Samples were irradiated with monochromatized CuKα radiation (1.542 Å) and analyzed at 5 to 30°2θ, step size: 0.02, time per step: 2 s. The voltage and current used were 30 kV and 30 mA, respectively.

In-vitro Deposition Study in Cascade Impactor

SS was mixed separately with 63–90 μm size fractions of different lactose batches and Pharmatose in a ratio of 1:67.5, *w*/*w* in accordance with the ratio employed in the commercial Ventolin® formulations. The blending was carried out by sequential mixing of lactose particles (63–90 μm size fractions) of each batch to SS in stoppered vials placed on a vibromixer for 5 s till the desired ratio of 1:67.5 was obtained followed by final blending in a fabricated double cone blender for 30 min at 40 rpm. Content uniformity was determined across each blend by analyzing the samples for SS content by UV spectrophotometry (UV-1601, Shimandzu Corporation, Japan) at 276 nm. Hard gelatin capsules (size "3") were filled manually with 33.0±1.5 mg of the powder mixture so that each capsule contained 481±20 μg SS, which was similar to the unit dose contained in a Ventolin Rotacap®.

The dispersion behavior of the powders was assessed using an eight stage, nonviable Anderson cascade impactor with a preseperator (Graseby-Anderson, Atlanta, GA, USA) operating at an flow rate of 28.3 l/min measured with a rotameter (Gilmont, USA, GF-2005). The powder samples in capsules were aerosolized using Rotahaler® (Cipla ltd, Mumbai, India). SS deposited at different locations was also assayed by UV spectrophotometry at 276 nm. A variety of parameters were employed to characterize the deposition profiles of SS. The recovered dose (RD) is the sum of the drug collected from capsule, inhaler device, pre-separator, induction port and all stages of the impactor. The emitted dose (ED) is the amount of drug released from the inhaler device, i.e. the sum of drug collected at preseperator, induction port and all stages of the impactor. FPD was defined as the amount of drug deposited on the stages 2 and below of the impactor. The FPF and dispersibility were calculated as the ratio of FPD to RD and ED, respectively. The total recovery (% recovery) of the drug was assessed by the ratio of the RD to the theoretical dose of SS in one capsule (481±22 μg), which was equivalent to the filling weight of SS and lactose blends (33.0±1.5 mg).

RESULTS AND DISCUSSION

α-LM employed as carrier for DPI is usually required to have size between 63–90 μm and high crystallinity, elongation ratio and surface smoothness. Rate of crystallization is known

Table II. Shape Descriptors, Density, CI and Angle of Repose of Different Lactose Batches

Batch code	Surface factor[a]	Elongation ratio[a]	Bulk density (g/cm^3)[b]	CI[b]	Angle of repose (°)[b]
Pharmatose	0.73±0.06	1.68±0.07	0.74±0.02	26±1	42±1
CC-1	0.72±0.07	1.68±0.05	0.73±0.03	25±1	43±2
CC-2	0.70±0.06	1.71±0.06	0.72±0.01	26±1	43±1
CC-3	0.68±05	1.73±0.07	0.75±0.04	27±1	44±1
Sono-1	0.71±0.08	1.83±0.05	0.57±0.02	29±1	48±1
Sono-2	0.69±0.03	1.94±0.04	0.57±0.02	31±2	48±1
Sono-3	0.67±0.07	2.10±0.06	0.56±0.01	32±1	47±1
Sono-S1	0.66±0.08	2.16±0.05	0.72±0.02	34±1	41±1
Sono-S2	0.64±0.06	2.21±0.07	0.75±0.03	35±1	42±2
Sono-S3	0.63±0.06	2.27±0.06	0.73±0.04	37±2	43±1
Sono-G1	0.76±0.02	2.48±0.04	0.74±0.03	21±2	37±1
Sono-G2	0.76±0.04	2.52±0.06	0.74±0.02	22±1	38±1
Sono-G3	0.75±0.03	2.69±0.05	0.72±0.05	22±1	38±0

Mean ± SD
[a] n=50
[b] n=6

to influence the crystal habit. The major factor governing the rate of lactose crystallization is the supersaturation, which increases with concentration. Therefore, preliminary experiments were carried out to understand the effect of variables and their levels on rate of crystallization. Lactose solutions with various concentrations (30%, 40% and 50% *w*/*w*) were prepared and effect of crystallization with and without sonication on crystal habit was studied. In absence of sonication the nuclei induction as well as crystal growth was extremely slow and hence, the crystals were allowed to grow for longer time till the desired size is achieved. Time of sonication influence final crystal size hence; the sonication time was varied. As the growth in stagnant and stirring conditions is known to result in different crystal habit, two different post sonication treatments were studied. Crystallization conditions for different batches are specified in Table I.

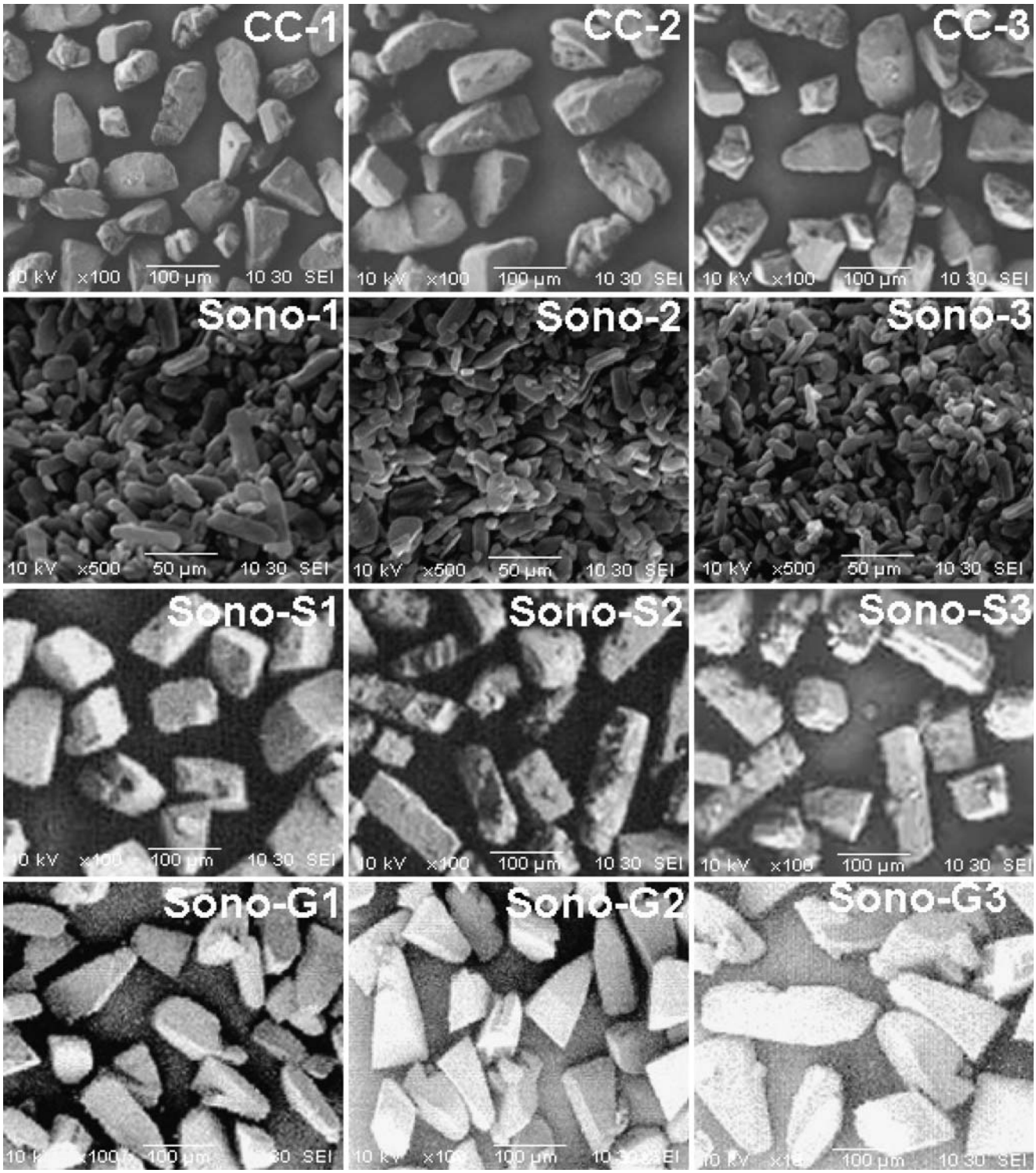

Fig. 1. SEM photomicrographs of different lactose batches.

Particle Size and Morphology

Cooling crystallization under constant stirring from lactose solutions of different concentration resulted in varied crystal size, shape and surface texture (Tables I, II and Fig. 1). The induction times as long as 3–10 h with crystallization times ranging from 8–20 h were required to reach D_{90} of 85–100 μm. The yield varied with the lactose concentration from 44% to 53% *w*/*w*. Further, these particles exhibited wide span as well as PSD, resulting in a relatively small fraction of crystals in the desired size range (63–90 μm). The crystal shape also varied with initial lactose concentration. Lower concentrations favored formation of tomahawk shaped crystals, while higher concentrations favored slightly elongated crystals. The results were in accordance with earlier reports (24). As reported by Zeng *et al.*, pre-washing with 60% ethanol was found to be essential before washing with 100% ethanol (22). After separation from mother liquor, the crystals still had traces of mother liquor adhered to the surface. If the crystals were directly washed with 100% ethanol, the lactose remaining in solution crystallized spontaneously in to needle shaped fine crystals. Pre-washing with lower ethanol concentration removes most of the mother liquor from the crystal surface without the formation of unwanted crystals. However, washing with too lower ethanol concentrations results in erosion of crystal surface or dissolution of entire crystal. Therefore, all batches were pre-washed with 60% ethanol before washing with 100% ethanol.

Sonocrystallization showed very rapid nuclei induction and crystal growth. Though exact time of nucleation could not be monitored, the induction can be assumed to appear rapidly from the turbidity observed by naked eye immediately after insonation for 30 s. The complete process of crystallization was over in 5 min with ~84% yield. It was interesting to note that nuclei induction, growth rates and yield were not very sensitive to lactose concentration. When ultrasound propagates through a liquid medium, its power is not only a driving force for mass transfer, but also initiates an important phenomenon known as cavitation. When a cavitational bubble implodes, a localized hot spot is formed with a high temperature and pressure releasing a powerful shock wave. This cavitation generates high local supersaturation leading to spontaneous nucleation in otherwise unsaturated liquid (30–32). The acoustic streaming, micro streaming and highly localized temperature and pressure within the fluid causes spontaneous induction of primary nucleation, reduction of crystal size, inhibition of agglomeration and manipulation of crystal size distribution (16,17,25). Sono-1, Sono-2 and Sono-3 showed rod-shaped lactose crystals (Fig. 1) with significantly (ANOVA, $P<0.01$) high elongation ratio compared with CC batches (Table II). This was attributed to the inherent differences in the crystal growth rates, leading to some crystal faces growing faster than other (33). Rapid crystallization of lactose is known to accelerate the growth of longest axis of the crystals at the expense of an increase in width and thickness resulting in needle-shaped elongated crystals (13, 24). Particles in size range of 15–30 μm and narrow PSD were obtained for these batches (Table I). Due to rapid supersaturation and nucleation achieved throughout the vessel, the number of primary nuclei increased and the amount of solute depositing on each primary nucleus decreased resulting in fine crystals. These results were in accordance with our previous report where we were able to generate nanoparticles by ultrasound assisted sonoprecipitation (34). Sono-1, Sono-2 and Sono-3 particles are fine and not suitable as DPI carrier. However, these particles may have find application as diluents in preparation of tablets by wet-granulation or when milling is carried out during processing, since fine size permits better mixing with other ingredients (5).

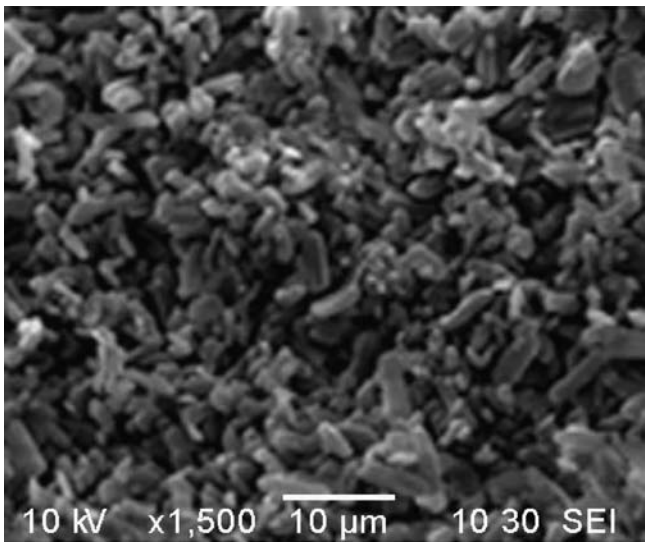

Fig. 2. SEM photomicrograph of seed crystals harvested after sonication for 45 s.

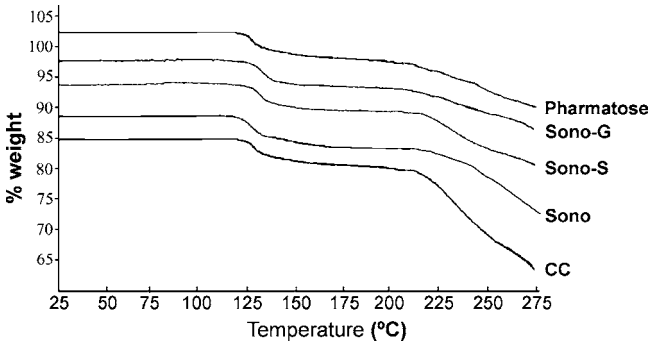

Fig. 3. TGA thermograms of different lactose batches.

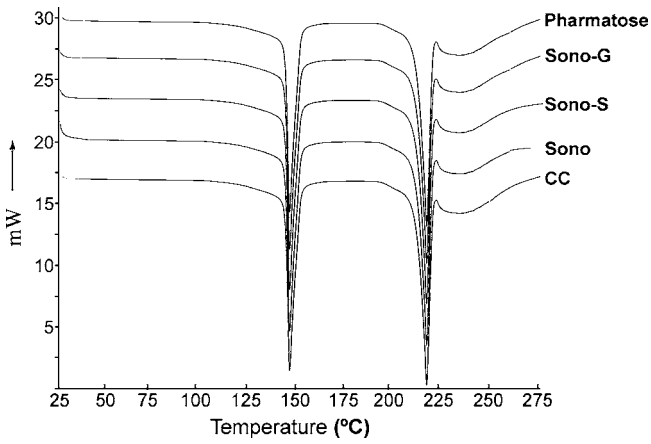

Fig. 4. DSC thermograms of different lactose batches.

Table III. Enthalpy of Dehydration and Moles of Water of Crystallization per Mole of Anhydrous Lactose of Different Lactose Batches and Pharmatose

Batch code	Enthalpy of dehydration (w/g)	Moles of water/mole of anhydrous lactose
Pharmatose	120.14±0.96	1.06±0.04
CC	116.02±1.11	1.02±0.03
Sono	112.52±1.03	0.99±0.02
Sono-S	118.23±1.02	1.04±0.01
Sono-G	121.31±1.05	1.07±0.01

The values are obtained from DSC thermograms. Mean ± SD, n=3

In Sono-S and Sono-G batches, sonication was used for *in-situ* seeding and discontinued after 45 s to yield rod-shaped fine seed crystals (<5 μm) (Fig. 2). Seeds were allowed to grow either under stirring (Sono-S1, Sono-S2 and Sono-S3) or in viscous glycerin solution (Sono-G1, Sono-G2 and Sono-G3) (Table I). Sono-S and Sono-G batches require 3 and 5 h, respectively to grow up to D_{90} of 78–81 μm (Table I). The crystals of sono-S and sono-G batches give 74 to 79% product yield (Table I) and exhibit significantly (ANOVA, P<0.001) high elongation ratios compared with CC batches (Table II). Rod-shaped morphologies of seed crystals might be responsible for high elongation ratio of these batches as seeding crystallization generally shows epitaxial growth, where seeds crystallize isomorphously with the native crystals and hence share same structural features as the substrate like crystal shape (15).

Sono-S batches showed rough surface, while surface of sono-G batches was smooth. (Fig. 1). This observation was supported by significantly (ANOVA, P<0.001) higher values of surface factor for Sono-G batches than Sono-S and CC batches (Table II). This was attributed to the difference in post sonication treatment. Mechanical stirring introduces random fluctuations in the solution and cause heterogeneous distribution of local concentrations, leading to uneven growth of crystals with surface irregularities or crevices. As stagnant conditions are known to have better control on crystallization, avoiding surface imperfections, the elongation ratio as well as the surface factor of Sono-G crystals improved. Moreover, the values of surface factor, span and PSD were consistent for Sono-G batches suggesting suppressed sensitivity of PSD and crystal shape to initial lactose concentration. Lactose molecules can be expected to diffuse freely in the medium under constant stirring and hence, any change in the supersaturation changes the crystallization pressure in the vicinity of the growing crystals, eventually changing the crystal shape as observed in Sono-S batches. However, after addition of glycerin (20% *w*/*w* final concentration) the viscosity of solution increased from 1.01 to 1.91 mPa s. The viscosities were determined by Brookfield programmable viscometer, Model-DV-II (Brookfield Engineering Labs. Inc., Stoughton, MA 02072, USA.). This increased viscosity imposes a resistance for free diffusion of lactose molecules, maintaining concentrations in the immediate vicinity of the growing crystals lower than the apparent concentration in the bulk of the crystallization medium. Therefore, any increase in the apparent supersaturation of lactose may not result in a corresponding increase in the effective concentration driving crystal growth. This would result in a reduction in the sensitivity of crystal habit to lactose concentration. Further, the viscous medium permits a steady diffusion of crystallizing molecules without introducing any external turbulence providing a homogeneous environment in which the crystals grow to maturity without any surface defects. This resistance for free diffusion of crystallizing molecules is also responsible for slightly lower yield of 'G' batches compared to 'S' batches where molecules diffuse freely under stirring. Secondary or heterogeneous nucleation is also suppressed compared to solution under agitation resulting in large crystals with narrow PSD and span.

Powder Flow

Powder flow was examined using static (Carr's compressibility index, CI) and dynamic methods (angle of repose). Bulk densities of all lactose batches were comparable except Sono-1, Sono-2 and Sono-3, which exhibited lower bulk densities due to smaller crystal size. The values of CI and angle of repose for all batches are given in Table II. CI values traditionally provide an estimate of the powder flow as discrete particles. Lower values of CI and angle of repose are indicative of good flow. Sono-G1, Son-G2 and Sono-G3 crystals showed more consistent and lowest values of CI and angle of repose, while Sono-S1, Sono-S2 and Sono-S3 crystals showed highest values. The magnitude of van der Waals forces increase with reducing particle size, due to reduced separation

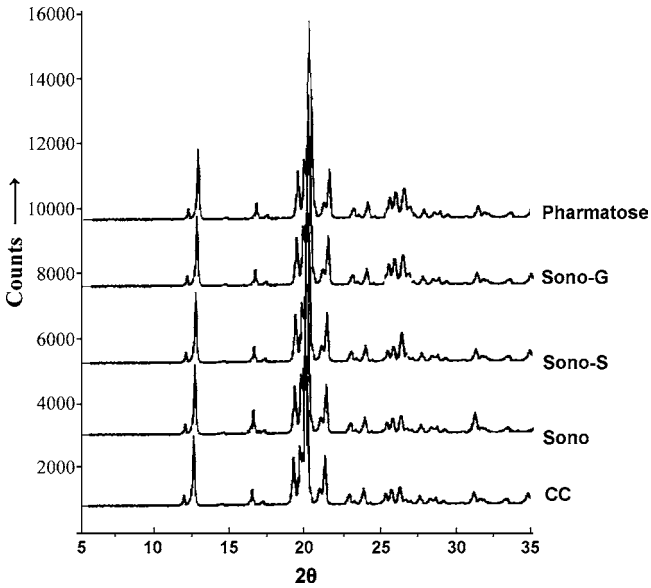

Fig. 5. XRPD profiles of different lactose batches.

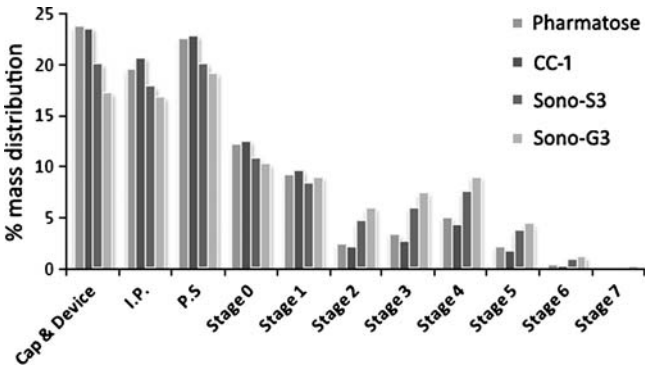

Fig. 6. Drug deposition profiles of blends containing different lactose batches in Anderson cascade impactor at 28.3 l/min via Rotahaler®.

distance between particles and weaker gravitational forces showing poor powder flow as observed in Sono-1, Sono-2 and Sono-3. Large crystal size of Sono-S and Sono-G batches (67–98 μm) experience low van der Walls forces exhibiting good flow. However, Sono-G batches show better flow than Sono-S batches. This might be due to smooth surface which reduces electrostatic forces and internal friction during flow. Since, powder flow is important in DPI formulations during capsule filling as well as subsequent release of drugs, Sono-G batches might prove beneficial as DPI carrier.

Characterization of Polymorphic Form

All recrystallized lactose samples showed TGA data typical of α-LM (Fig. 3). Weight loss between 120°C and 190°C was due to loss of water of crystallization and not due to vaporization of free water, which generally occurs at 100°C. Weight loss at 200–250°C may be due to decomposition of lactose. Dehydration of 4.5–5.5% *w/w* was observed in all samples, indicating presence of 1 mol of water of crystallization per mol of anhydrous lactose. Dehydration of water of crystallization was also observed in DSC thermograms at about 130°C followed by the melting endotherm typical of α-LM at 217°C and a broad endothermic peak around 240°C due to thermal degradation (Fig. 4). Charring was confirmed by visual examination at the end of DSC run. Absence of an exothermic crystallization peak around 177°C in the DSC scans of all samples indicates highly crystalline nature. The number of moles of water per mole of anhydrous lactose (n) was calculated from the values of enthalphy of dehydration obtained from DSC thermograms using Eq. 5 as reported by Khankari *et al.* (35):

$$n = \frac{\Delta H_d \times \mathrm{RMM}_{\mathrm{lactose}}}{(\Delta H_v - \Delta H_d) \times \mathrm{RMM}_{\mathrm{water}}} \quad (5)$$

where, ΔH_d is the enthalpy of dehydration obtained from the dehydration endotherm (joules per gram); ΔH_v is the enthalpy of vaporization of water, 2,261 J/g (36), and $\mathrm{RMM}_{\mathrm{lactose}}$ and $\mathrm{RMM}_{\mathrm{water}}$ are the relative molecular masses of anhydrous lactose (340.3) and water (18.0), respectively. All recrystallized lactose batches appear to contain ~1 mol of water of crystallization per mol of anhydrous lactose (Table III) which was in accordance with the results of TGA and confirmed the presence of α-LM form.

X-ray diffractogram of crystalline lactose has a distinct peak at 19–20°2θ as main signal, with minor peaks at different angles depending on the isomer, with α-lactose at 12.6° and β-lactose at 10.5° (37). The major peaks of all recrystallized lactose carriers were consistent with those of α-lactose and the presence of β-lactose was not detected (Fig. 5). Slight variations in peak intensities between samples may be due to preferred orientation and minor differences in the degree of crystallinity.

In-vitro Aerosol Deposition Studies

Micronized SS was blended separately with 63–90 μm sieved fraction of different lactose batches in a ratio of 1:67.5 and filled in hard gelatin capsule. The content uniformity ranged from 95.83% to 101.42% for all samples. The *in-vitro* aerosol deposition studies were carried out in cascade impactor using Rotahaler® at 28.3 l/min. The drug recovery for various formulations ranged from 86.69% to 95.63%, which was within the acceptable range (75–125%) for mass balance (38) and also suggested that the method of washing and analyzing was accurate and reproducible. The deposition profiles varied with the type of carrier lactose employed. Since the powders are composed of the same quantity of SS from same batch, the difference in the deposition profiles of the drug may largely be as a result of the differences in particle shape and surface of lactose carrier particles. The percent mass deposited on different stages of cascade impactor are shown in Fig. 6. Various formulations produced different deposition profiles of SS, which are summarized in Table IV.

The formulation containing CC-1 lactose produced lower dispersion of SS compared to formulation containing Pharmatose (Table IV), since most of the emitted dose of SS was deposited in preseperator and induction port, allowing only small fraction of drug to reach lower stages (Fig. 6). Approximately 30% of the drug released from this formulation was retained in the capsule and the device. This was evidenced by concomitantly lower FPF (11.03%) of the drug. Despite similar values of elongation ratio, formulation containing Pharmatose produced slightly higher FPF (13.01%) than CC-1. This could be due to the fact that the commercial

Table IV. Deposition of Salbutamol Sulphate from Different Lactose Batches in Anderson Cascade Impactor at 28.3 l/min Via Rotahaler®

Batch no.	RD (μg)	ED (μg)	FPD (μg)	FPF (%)	Recovery (%)	Emission (%)
Pharmatose	426 (16)	325 (14)	55 (11)	13.01 (1.6)	88.66 (1.6)	67.00 (2.1)
CC-1	417 (16)	319 (14)	46 (11)	11.03 (1.6)	86.69 (1.7)	66.32 (2.1)
Sono-S3	453 (11)	362 (10)	103 (7)	22.82 (1.3)	94.28 (1.6)	75.36 (1.4)
Sono-G3	460 (13)	381 (12)	128 (8)	27.82 (1.5)	95.63 (1.3)	79.20 (1.6)

Mean (SD), n=3

Pharmatose might have undergone size reduction processing during manufacture generating fines. These fines might have adhered on the surface crevices and asperities of the carrier lactose which are known to reduce the adhesive forces between the carrier surface and drug improving the de-agglomeration behavior (39). Therefore, CC-1 lactose prepared under similar condition was used as control batch.

Formulations containing Sono-S3 and Sono-G3 lactose showed better deposition profiles than the control lactose formulations. Sono-G3 lactose produced highest FPF; 27.82± 1.5% and RD; 460±13 μg of drug followed by Sono-S3 lactose with FPF; 22.82±1.3% and RD; 453±11 μg of drug. The difference in the deposition profiles from different formulations could be attributed to the difference in the morphological features like elongation ratio and surface smoothness. This can be explained by the fact that elongated particles have aerodynamic diameters almost independent of their length and is governed by the shorter dimension of the particle (40,41). Such particles exhibit smaller aerodynamic diameters than spherical particles of similar mass or volume (42). More elongated particles may also be expected to travel a longer distance before impaction occurs in comparison to less elongated particles of similar mass, as a result of lower relative aerodynamic diameters of the former. More drug particles can adhere to elongated carrier particles in comparison to spherical particles. Elongated particles are also known to experience drag forces of the air stream for longer period of time. This would be expected to result in a higher proportion of drug being detached from the carrier particle leading to a higher FPF of the drug (22). In spite of slight difference in the elongation ratio, Sono-S2 produced lower FPF than Sono-G2, which could be attributed to the difference in the surface smoothness. Sono-S has showed rough surface as indicated by the lower values of surface factor (Table II) and SEM images (Fig. 1). Thus, the microscopic asperities might have acted as adhering sites for drug preventing the de-agglomeration from its surface. However, growth of lactose crystals in viscous glycerin medium permits a steady diffusion of crystallizing molecules without any external turbulence providing a homogeneous environment in which the Sono-G crystals grow to maturity without surface defects. Therefore, high elongation ratio and surface factor of Sono-G3 batch was responsible for highest FPF.

CONCLUSION

Sonocrystallization offers spontaneous supersaturation resulting in early nucleation. Spontaneous nucleation and growth of seeds accelerate the growth of length rather than the width and thickness resulting in rod shaped seed crystals. These seed crystals are delicately held in their position in glycerin while the growth proceeds in homogeneous environment without introducing any external turbulence into large elongated crystals with smooth surface. Owing to the rod-shaped morphology of the seeds produced by sonication, the crystals grown under stirring as well as in glycerin showed high elongation ratio. Formulation containing Sono-G3 crystals with high elongation ratio and surface factor produced highest dispersibility and FPF. It can be concluded that ultrasound assisted *in-situ* seeding, followed by ordered growth in glycerin offers rapid crystallization technique for engineering α-LM crystals with higher elongation ratio, smooth surface and better flow. All these factors are responsible for improving the dispersion and FPF of adhered drug, which might serve as viable means of improving drug delivery to the lower airways from DPIs.

ACKNOWLEDGEMENTS

Anant R. Paradkar is thankful to British Council for UK-India Education and Research Initiative (UKERI) Fellowship, Bharati Vidyapeeth University, Pune for the sabbatical leave and AICTE (New Delhi, India) for grant in the form of Research Promotion Scheme. Ravindra S. Dhumal and Shailesh V. Biradar are thankful to CSIR (New Delhi, India) for providing financial support in the form of Senior Research Fellowship (SRF). Authors acknowledge the support of Cipla Ltd, (Mumbai, India), DMV International (The Netherlands) and Universal Capsules (Mumbai, India) for providing gift samples of salbutamol sulphate, lactose monohydrate and hard gelatin capsules, respectively. Authors are thankful to Dr. P. K. Khanna, Head, Nano Science group, Centre for Materials for Electronic Technology (C-MET), Pune, India for providing the facilities at C-MET.

REFERENCES

1. V. Kapil, A. K. Dodeja, and S. C. Sharma. Manufacture of lactose—Effect of processing parameters on yield and purity. *J. Food Sci. Tech*. **28**:167–170 (1991).
2. T. A. Nickerson. Lactose chemistry. *J. Agri. Food Chem.* **27**:672–677 (1979) doi:10.1021/jf60224a038.
3. B. Elvers, S. Hawkins, and G. Schulz. *Ullmann's encyclopedia of industrial chemistry. Vol. A, 15*. VCH, Germany, 1990, pp. 107–114.
4. H. G. Brittain, S. J. Bogdanowich, D. F. Bugay, J. DeVincentis, G. Lewen, and A. W. Newman. Physical characterization of pharmaceutical solids. *Pharm. Res.* **8**:963–973 (1991) doi:10.1023/A:1015888520352.
5. A. H. Kibbe (Ed). Lactose. In *Handbook of pharmaceutical excipients*, 3rd Edn. London Pharmaceutical, London, 2000, pp. 276–285.
6. S. L. Raghavan, R. I. Ristic, D. B. Sheen, and J. N. Sherwood. The bulk crystallization of lactose monohydrate from aqueous solution. *J. Pharm. Sci.* **90**:823–832 (2000) doi:10.1002/jps.1036.
7. Y. Shi, B. Liang, and R.W. Hartel. Crystallization kinetics of alpha-lactose in a continuous cooling crystallizer. *J. Food Sci.* **55**:817–820 (1990) doi:10.1111/j.1365-2621.1990.tb05238.x.
8. B. Liang, Y. Shi, and R. W. Hartel. Growth rate dispersion effects on lactose crystal size distributions from a continuous cooling crystallizer. *J. Food Sci.* **56**:848–854 (1991) doi:10.1111/j.1365-2621.1991.tb05397.x.
9. R. K. Bund, and A. B. Pandit. Rapid lactose recovery from buffalo whey by use of 'anti-solvent, ethanol'. *J. Food Eng.* **82**:333–341 (2007) doi:10.1016/j.jfoodeng.2007.02.045.
10. H. Larhrib, G. P. Martin, C. Marriot, and D. Prime. The use of engineered lactose crystals as a carrier for aerosolized salbutamol sulphate from dry powder inhalers. *Proceedings of drug delivery to the lungs, London*. **10**:155–159 (1999).
11. A. Leviton. Methanol extraction of lactose and soluble proteins from skim milk powder. *Ind. Eng. Chem.* **41**:1351–1357 (1949) doi:10.1021/ie50475a013.
12. T. D. Dincer, G. M. Parkinson, A. L. Rohl, and M. I. Ogden. Crystallization of a-lactose monohydrate from dimethyl sufoxide (DMSO) solution: influence of b-lactose. *J. Cryst. Growth*. **205**:368–374 (1999) doi:10.1016/S0022-0248(99)00238-9.

13. H. Larhrib, G. P. Martin, D. Prime, and C. Marriot. Characterization and deposition studies of engineered lactose crystals with potential for use as a carrier for aerosolized salbutamol sulphate from dry powder inhalers. *Eur. J. Pharm. Sci.* **19**:211–221 (2003) doi:10.1016/S0928-0987(03)00105-2.
14. R. K. Bund, and A. B. Pandit. Sonocrystallization: effect on lactose recovery and crystal habit. *Ultrason. Sonochem.* **14**:143–152 (2007) doi:10.1016/j.ultsonch.2006.06.003.
15. T. Bergfors. Seeds to crystals. *J. Struct. Biol.* **142**:66–76 (2003) doi:10.1016/S1047-8477(03)00039-X.
16. M. Louhi-Kultanen, M. Karjalainen, J. Rantanen, M. Huhtanen, and J. Kallas. Crystallization of glycine with ultrasound. *Int. J. Pharm.* **320**:23–29 (2006) doi:10.1016/j.ijpharm.2006.03.054.
17. H. Li, J. Wang, Y. Bao, Z. Guo, and M. Zhang. Rapid sonocrystallization in the salting-out process. *J. Cryst. Growth*. **247**:192–198 (2003) doi:10.1016/S0022-0248(02)01941-3.
18. H. Steckel, P. Markefka, H. teWierik, and R. Kammelar. Functionality testing of inhalation grade lactose. *Eur. J. Pharm. Biopharm.* **57**:495–505 (2004) doi:10.1016/j.ejpb.2003.12.003.
19. X. M. Zeng, G. P. Martin, S. K. Tee, A. A. Ghoush, and C. Marriott. Effect of particle size and adding sequence of fine lactose on the deposition of salbutamol sulphate from dry powder formulation. *Int. J. Pharm.* **182**:133–144 (1999) doi:10.1016/S0378-5173(99)00021-6.
20. H. Larhrib, G. P. Martin, C. Marriot, and D. Prime. The influence of carrier and drug morphology on the drug delivery from dry powder formulation. *Int. J. Pharm.* **25**:283–296 (2003) doi: 10.1016/S0378-5173(03)00156-X.
21. J. N. Staniforth. Improvement in dry powder inhaler performance: surface passivation effects. *Proceedings of Drug Delivery to Lung*. **8**:85–86 (1997).
22. X. M. Zeng, G. P. Martin, C. Marriott, and J. Pritchard. Crystallization of lactose from carbopol gels. *Pharm. Res.* **17**:879–886 (2001) doi:10.1023/A:1007572612308.
23. X. M. Zeng, G. P. Martin, C. Marriott, and J. Pritchard. The use of lactose recrystallised from carbopol gels as a carrier for aerosolised salbutamol sulphate. *Eur. J. Pharm. Biopharm.* **51**:55–62 (2001) doi:10.1016/S0939-6411(00)00142-9.
24. X. M. Zeng, G. P. Martin, C. Marriott, and J. Pritchard. The influence of crystallization conditions on the morphology of lactose intended for use as a carrier for dry powder aerosols. *J. Pharm. Pharmacol.* **52**:633–643 (2000) doi:10.1211/0022357001774462.
25. M. D. Luque de Castro, and F. Priego-Capote. Ultrasound-assisted crystallization (sonocrystallization). *Ultrason. Sonochem.* **14**:717–724 (2007) doi:10.1016/j.ultsonch.2006.12.004.
26. M. N. Patil, G. M. Gore, and A. B. Pandit. Ultrasonically controlled particle size distribution of explosives: a safe method. *Ultrason. Sonochem.* **15**:177–187 (2008) doi:10.1016/j.ultsonch.2007.03.011.
27. M. Maheshwari, H. Jahagidar, and A. R. Paradkar. Melt sonocrystallization of ibuprofen: effect on crystal properties. *Eur. J. Pharm. Sci.* **25**:41–48 (2005) doi:10.1016/j.ejps.2005.01.013.
28. A. R. Paradkar, M. Maheshwari, R. Kamble, I. Grimsey, and P. York. Design and Evaluation of celecoxib porous particles using melt sonocrystallization. *Pharm. Res.* **23**:1395–1400 (2006) doi:10.1007/s11095-006-0020-4.
29. A. R. Paradkar, M. Maheshwari, A. R. Ketkar, and B. Chauhan. Preparation and evaluation of ibuprofen beads by melt solidification technique. *Int. J. Pharm.* **255**:33–42 (2003) doi:10.1016/S0378-5173(03)00081-4.
30. Z. Guo, A. G. Jones, and N. Li. The effect of ultrasound on the homogeneous nucleation of BaSO4 during reactive crystallization. *Chem. Eng. Sci.* **61**:1617–1626 (2006) doi:10.1016/j.ces.2005.09.009.
31. Z. Guo, A. M. Zhang, and H. Li. The effect of ultrasound on anti-solvent crystallization process. *J. Cryst. Growth*. 273:555–563 (2005) doi:10.1016/j.jcrysgro.2004.09.049.
32. P. W. Cains, P. D. Martin, and C. J. Price. The use of ultrasound in industrial chemical synthesis and crystallization. 1. Application to synthetic chemistry. *Org. Process Res. Dev.* **2**:34–48 (1998) doi:10.1021/op9700340.
33. A. van Kreveld, and A. S. Michaels. Measurement of crystal growth rates in lactose crystals. *J. Dairy Sci.* **38**:107–133 (1965).
34. R. S. Dhumal, S. V. Biradar, S. Yamamura, A. R. Paradkar and P. York. Preparation of amorphous cefuroxime axetil nanoparticles by sonoprecipitation for enhancement of bioavailability. *Eur. J. Pharm. Biopharm.* (2008) doi:10.1016/j.ejpb.2008.04.001.
35. R. K. Khankari, D. Law, and D. J. W. Grant. Determination of water content in pharmaceutical hydrates by differential scanning calorimetry. *Int. J. Pharm.* **89**:117–127 (1992) doi:10.1016/0378-5173(92)90080-L.
36. J. G. Stark and H. G. Wallace. In: *Chemistry data book*, SI Edn. John Murry, London, 1976, pp. 122.
37. G. Buckton, O. C. Chidavaenzi, and F. Koosha. The effect of spray drying feed temperature and subsequent crystallization conditions on the physical form of lactose. *AAPS PharmSciTech.* **3**:1–6 (2002) doi:10.1208/pt0304.
38. P. R. Bryon, E. L. Kelly, and M. J. Kontny. Recommendations of the USP Advisory Panel on aerosols on the USP general chapters on aerosols <601> and uniformity of dosage units <905>. *Pharm. Forum*. **20**:7477–7505 (1994).
39. X. M. Zeng, G. P. Martin, S. K. Tee, and C. Marriott. The role of fine lactose on the dispersion and deaggregation of salbutamol sulphate in an air stream *in vitro*. *Int. J. Pharm.* **176**:99–110 (1998) doi:10.1016/S0378-5173(98)00300-7.
40. W. C. Hinds. Aerosol technology: properties, behavior and measurement of airborne particles. Wiley Interscience, New York, 1982.
41. K. Ikegami, Y. Kawashima, H. Takeuchi, H. Yamamoto, N. Isshiki, D. Momose, and K. Ouchi. Improved inhalation behavior of steroid KSR-592 *in vitro* with JethalerÒ by polymorphic transformation to needle-like crystals (b-form). *Pharm. Res.* **19**:1439–1445 (2002) doi:10.1023/A:1020492213172.
42. A. J. Hickey, K. A. Fults, and R. S. Pillai. Use of particle morphology to influence the delivery of drugs from dry powder aerosols. *J. Biopharm. Sci.* **3**:107–113 (1992).